Monomorphic epitheliotropic intestinal T-cell lymphoma with gallbladder involvement: A case report

TAKEHIRO OKUDA[1], TOMOYUKI SHIRASE[2], MASASHI NISHIKUBO[3], YUKI KONISHI[1], TOMOHARU TAKEOKA[1], JUN TAKESHIMA[4], TATSUO ITO[4] and MASAAKI TSUJI[1]

[1]Department of Hematology, Otsu Red Cross Hospital, Otsu, Shiga 520-8511, Japan; [2]Department of Pathology, Otsu Red Cross Hospital, Otsu, Shiga 520-8511, Japan; [3]Department of Hematology, Kobe City Medical Center General Hospital, Kobe, Hyogo 650-0047, Japan; [4]Department of Surgery, Otsu Red Cross Hospital, Otsu, Shiga 520-8511, Japan

Received August 22, 2024; Accepted April 17, 2025

DOI: 10.3892/mco.2025.2862

Abstract. Monomorphic epitheliotropic intestinal T-cell lymphoma (MEITL) is a rare and aggressive primary intestinal lymphoma with a poor prognosis. MEITL can metastasize to the central nervous system, liver and spleen, but gallbladder involvement has not yet been reported. The present study describes the case of a 57-year-old woman who presented with abdominal distention, pain and vomiting. Contrast-enhanced computed tomography revealed thickening and perforation of the small intestinal wall, and a gallbladder mass. Histopathological analysis of the affected small intestine and gallbladder revealed a dense infiltrate of medium-sized monomorphic lymphocytes with a $CD3^+$, $CD4^-$, $CD8^+$ and TIA-1^+ phenotype. Based on the absence of celiac disease, aggressive clinical course, and characteristic histopathological and immunophenotypic features, a diagnosis of MEITL with gallbladder involvement was established. The patient underwent small intestinal resection and cholecystectomy, followed by chemotherapy, which was completed without gastrointestinal or gallbladder perforation. Diagnostic resection is currently the best approach for suspected malignant lymphoma of the gallbladder. This rare case of MEITL with gallbladder involvement highlights the importance of considering this diagnosis in similar clinical scenarios and the role of cholecystectomy, which can serve both diagnostic and therapeutic purposes.

Introduction

Monomorphic epitheliotropic intestinal T-cell lymphoma (MEITL), previously designated as type 2 enteropathy-associated T-cell lymphoma (EATL), is an uncommon primary intestinal lymphoma originating from intestinal intraepithelial T lymphocytes (1,2). Unlike classical EATL, MEITL is not associated with celiac disease and is more frequently seen in East Asian populations. Histologically, MEITL is characterized by medium-sized monomorphic lymphocytes with a cytotoxic immunophenotype, typically $CD3^+$, $CD4^-$, $CD8^+$ and TIA-1^+ (2,3). MEITL is characterized by rapid progression and poor prognosis, attributed to therapeutic resistance and complications such as intestinal perforation or obstruction amid treatment, with a 5-year survival rate of approximately 20% and a 5-year relapse-free survival rate of only 4% (1). Treatment is challenging as chemotherapy alone is rarely curative, although autologous transplantation combined with high-dose chemotherapy has been shown to be effective (2,3).

MEITL lesions are predominantly located in the jejunum and ileum and typically manifest as gastrointestinal perforation or obstruction (1-3). Prior studies have documented metastatic lesions in the central nervous system, liver, and spleen, whereas no cases of gallbladder involvement have been reported (4). Herein, we present a case of MEITL with concurrent intestinal and gallbladder involvement, and highlights the diagnostic and therapeutic relevance of surgical resection.

Case report

A 57-year-old woman with a 2-week history of abdominal distention was admitted to Otsu Red Cross Hospital (Otsu, Japan) on January 2023, owing to abrupt-onset abdominal pain and vomiting. On physical examination, she had notable abdominal distension and pronounced tenderness. She was bedridden, and her Eastern Cooperative Oncology Group (ECOG) performance status was 3. Laboratory tests revealed leukocytopenia (white blood cell count, 2,600/μl; neutrophils, 85%; lymphocytes, 10%; monocytes, 5.0%; eosinophils, 0%; basophils. 0%), but no abnormal lymphocytes were detected on the peripheral blood smear. Thrombocytosis ($47.4x10^4/\mu l$), low total protein (6.1 g/dl), hypoalbuminemia (1.9 g/dl), elevated levels of C-reactive protein (9.2 mg/dl), and soluble interleukin-2 receptor (3,274 U/ml) were noted; lactate dehydrogenase levels were within the normal range (Table I). Contrast-enhanced computed tomography (CT) showed circumferential thickening and perforation of the jejunum

Correspondence to: Dr Masaaki Tsuji, Department of Hematology, Otsu Red Cross Hospital, 1-1-35 Nagara, Otsu, Shiga 520-8511, Japan
E-mail: shall2510@yahoo.co.jp

Key words: monomorphic epitheliotropic intestinal T-cell lymphoma, lymphoma, gallbladder, cholecystectomy

wall. In addition, a gallbladder mass and wall thickening were observed, with enlargement of the surrounding lymph nodes (Fig. 1A and B).

Based on all findings, emergency surgery was performed on the day of admission. Intraoperatively, we observed swelling of the jejunum with a 2-cm perforation and a mass located at the gallbladder neck with adhesions to the liver. The affected site of the small intestine was fused to the large mesentery and transverse colon, and the perforated area was resected. The gallbladder had severe adhesions owing to inflammation, and there were concerns that its removal could damage the bile duct. To avoid complications, we decided to preserve the gallbladder in the first surgery. Although the raw sample of the jejunum mass was submitted for flow cytometry, it was assessed to be unsuitable for the analysis and could not be analyzed.

For the histological analysis, the biopsied specimens were fixed in 10% buffered formalin for 24 h at room temperature (RT) and embedded in paraffin. Sections with a thickness of 4 μm were prepared from the paraffin block and stained with hematoxylin for 5 min and eosin for 1 min at RT. Immunohistochemistry (IHC) for CD3, CD8, CD4, CD5, CD20, CD56, TIA-1 and EBER-ISH was performed on 4 μm-thick sections obtained from the paraffin block using primary antibodies (Table II). IHC staining was conducted using automated immunostaining devices, VENTANA BenchMark ULTRA (Roche) and Histostainer 48A (Nichirei). Briefly, before staining, to block endogenous peroxidases, the IHC device-dedicated reagent (ultra View DAB universal; Roche Tissue Diagnostics) was used in CD3, CD4, CD8, CD5, CD20, CD56, TIA-1 staining; their temperature/duration were 36˚C/4 min and RT/5 min, respectively. In the deparaffinization process, EZ prep (Roche Tissue Diagnostics) was used. For EBER-ISH, *in situ* hybridization was carried out using a digoxigenin-labeled probe specific for Epstein-Barr virus-encoded RNA, with signal detection via anti-digoxigenin antibodies and subsequent chromogenic substrate application. The stained sections were then observed under a light microscope (BX53; Olympus Corporation).

Flow cytometry and Southern blotting were outsourced to SRL, Inc. (https://www.srl-group.co.jp/english/), a commercial testing company. Flow cytometry analysis was conducted on surgically removed samples. Immediately after excision, surgically removed samples were collected and maintained on ice (4˚C). The specimens were initially incubated in the dark at 4˚C for 5 min to stabilize the cell surface antigens. Following red blood cell lysis, the cells were resuspended in a cell preservation medium composed of 500 ml RPMI 1640, 25 ml 5% fetal bovine serum (FBS; cat. no. 164210-500; Procell Life Science & Technology Co., Ltd.), and 5 ml Penicillin-Streptomycin solution (cat. no. DXT-0503; ScienCell Research Laboratories, Inc.). After cell counting, the suspension was adjusted to a concentration of $3.0x10^6$ cells/ml. A total of 100 μl of the cell suspension was dispensed into each tube, followed by the addition of fluorochrome-conjugated monoclonal antibodies according to the antibody panel detailed in Table III. The samples were then incubated at 4˚C for 30 min in the dark to ensure optimal antigen-antibody binding. During the washing procedure, the cells were centrifuged at 400 x g for 5 min at 4˚C, the supernatant was carefully removed, and the cells were resuspended in cold PBS. This washing step was repeated three times. Appropriate staining controls (e.g., isotype and unstained controls) were included to validate the specificity of the staining and to guide the gating strategy. Finally, the cells were maintained at 4˚C in the dark and analyzed as soon as possible. Flow cytometry was performed using the FACSLyric system (BD Biosciences). Data acquisition and analysis were conducted following the prescribed protocol, with data analysis performed BD FACSDiva.

The Southern blot process was used to analyze specific DNA sequences from lymphoma tissue. Immediately after surgical removal, the tissue was frozen at -80˚C to preserve DNA integrity. Lymphoma cells were isolated from the frozen tissue, and genomic DNA was extracted using an automated system (WPC-1, Malcolm) and quantified for quality and yield. The DNA was then digested with restriction enzymes (e.g., *Hin*dIII or *Bam*HI, Roche Diagnostics) at 37˚C for about 2 h. The resulting fragments were separated on a 1% agarose gel (Agarose S, Fujifilm Wako) in TAE or TBE buffer at ~100 V for approximately 1 h. After electrophoresis, the gel was incubated in an alkaline solution (0.5 M NaOH with 1.5 M NaCl) at room temperature for 30 min to denature the DNA, which was then transferred onto a nylon membrane by capillary action. The DNA was immobilized by UV cross-linking with a spectrolinker (XL-1500, Nippon Genetics) at 120 mJ/cm^2. The membrane was pre-hybridized in a blocking solution (Blocking Reagent, Roche Diagnostics) at 42˚C for 1 h before being hybridized overnight at 42˚C in the MI 100 (Clabo) oven with a digoxigenin-labeled probe specific for lymphoma-related gene rearrangements. Following hybridization, the membrane was washed-first in 2X SSC with 0.1% SDS at room temperature and then in 0.1X SSC with 0.1% SDS at 65˚C for 15 min- to remove unbound probe. Specific signals were detected using anti-digoxigenin antibodies conjugated to alkaline phosphatase, followed by treatment with the chemiluminescent substrate CDP-Star. The emitted light was captured on X-ray film, which was developed using an automatic processor (MXP-2000, Kodak). Finally, the band sizes and intensities were compared with a molecular weight marker to determine the presence and structure of gene rearrangements characteristic of lymphoma.

Histopathological analysis of the resected jejunum revealed a dense infiltrate of medium-sized monomorphic lymphocytes with round nuclei and dispersed chromatin in all layers of the intestinal wall (Fig. 2A and B). Widespread infiltration was also seen in the mucosal layer near the jejunum mass, with intraepithelial infiltration and mucosal flattening. The unaffected area of the specimen showed no mucosal flattening, plasma cell infiltration, or other findings indicative of celiac disease. Upon immunostaining, the abnormal lymphocytes were positive for CD3, CD8, and TIA-1, and negative for CD4, CD5, CD20, CD56, and EBER-ISH. The Ki-67 proliferation index was approximately 40% (Fig. 2C-K). Background inflammatory cells, including normal T and B cells, were also present. CD4- and CD5-positive cells were interpreted as normal T cells, whereas CD20 positivity was indicative of B cells. However, distinguishing between normal T-cell and the T-cell tumor can be difficult. Immunostaining of TCR using immunohistochemistry (IHC) is challenging to perform under the Japanese insurance system. Therefore, it was not evaluated

Table I. Laboratory findings at the first visit.

Test	Result	Reference range
White blood cell, /μl	2,600	3,900-9,800
Neutrophil, %	85	40-75
Monocyte, %	5.0	2.0-10
Lymphocyte, %	10	18-49
Basophil, %	0.0	0.0-2.0
Eosinophil, %	0.0	0.0-8.0
Hemoglobin, g/dl	12.1	11.1-15.1
Platelet count, $x10^4/\mu l$	47.4	13.0-37.0
Total protein, g/dl	6.1	6.5-8.5
Albumin, g/dl	1.9	3.9-4.9
Total bilirubin, mg/dl	0.76	0.2-1.2
Aspartate aminotransferase, U/l	17	8-40
Alanine aminotransferase, U/l	15	8-40
Lactate dehydrogenase, U/l	148	124-222
Urea, mg/dl	17.2	8.0-20.0
Creatinine, mg/dl	0.61	0.40-0.80
C-reactive protein, mg/dl	9.2	0.00-0.50
Prothrombin time-international normalized ratio	0.98	
Activated partial thromboplastin time, sec	25.6	24.3-38.9
Soluble interleukin-2 receptor, U/ml	3,274	157-474
Human T-lymphotropic virus type 1 antigen	Negative	Negative

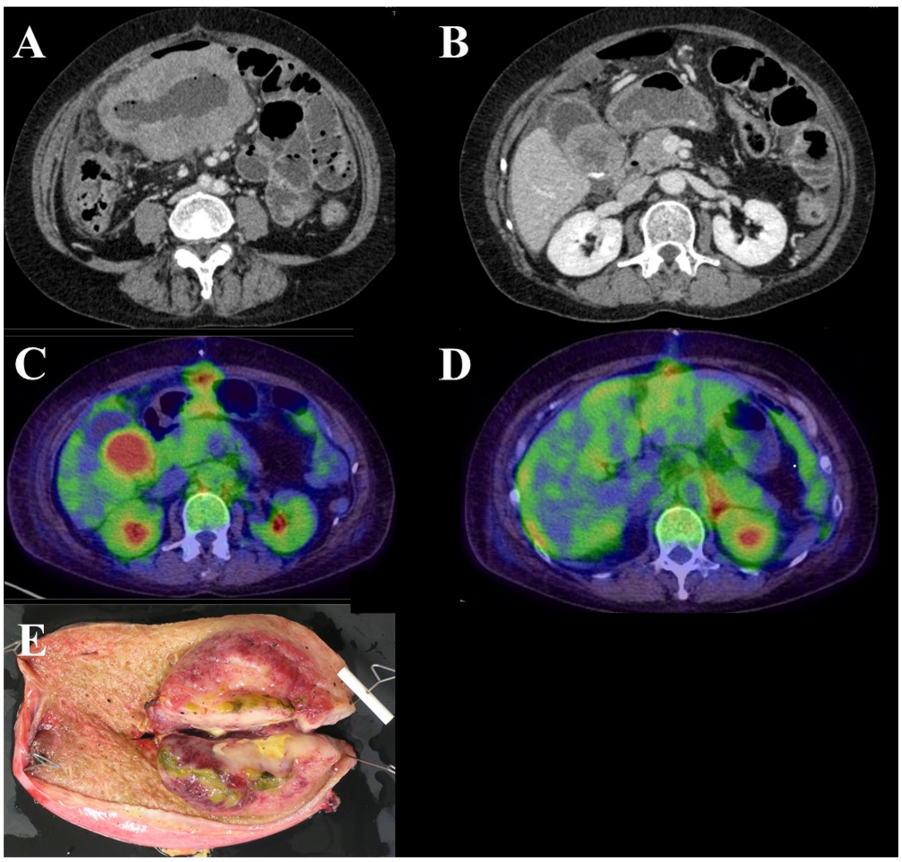

Figure 1. Imaging and postoperative pathological findings. (A) Computed tomography images showing localized wall thickening and perforation of the small intestine. (B) A gallbladder mass with wall thickening and enlarged regional lymph nodes. (C) Positron-emission tomography/computed tomography image showing radiotracer-avid lesions in the gallbladder. (D) The mesentery and left adrenal gland also showed FDG accumulation. (E) Postoperative specimen inspection following cholecystectomy showing a mass in the neck of the gallbladder. FDG, 18F-fluorodeoxyglucose.

Table II. Antibodies used for immunohistochemistry staining.

Antibody	Catalog number	Manufacturer
CD3	M7254	Dako
CD4	M7310	Dako
CD5	M3641	Dako
CD8	M7103	Dako
CD20	M0755	Dako
CD56	M7304	Dako
TIA-1	IM2550	Beckman
EBER-ISH	780-2842	Ventana

TIA-1, T-cell intracellular antigen-1; EBER-ISH, Epstein-Barr virus-encoded RNA-*in situ* hybridization.

Table III. Fluorochrome-conjugated monoclonal antibodies used for flow cytometry analysis.

Reagent name	Catalog number	Manufacturer
MsIgG (FITC)	340755	BD Biosciences
MsIgG (PE)	349043	BD Biosciences
CD2 (FITC)	555326	BD Biosciences
CD3 (PE)	555333	BD Biosciences
CD4 (APC-H7)	560158	BD Biosciences
CD5 (FITC)	347303	BD Biosciences
CD7 (APC)	561604	BD Biosciences
CD8 (BV510)	563256	BD Biosciences
CD10 (PE)	555375	BD Biosciences
CD11c (BV510)	563026	BD Biosciences
CD16 (BV510)	740203	BD Biosciences
CD19 (BV421)	562440	BD Biosciences
CD20 (APC-H7)	560853	BD Biosciences
CD23 (BV421)	562707	BD Biosciences
CD25 (BV421)	564033	BD Biosciences
CD30 (FITC)	555829	BD Biosciences
CD34 (APC)	555824	BD Biosciences
CD38 (APC)	555462	BD Biosciences
CD56 (APC)	555518	BD Biosciences
CD45 (PerCP)	347464	BD Biosciences
Kappa light chains (PE)	562052	BD Biosciences
Lambda light chains (APC-H7)	561325	BD Biosciences

MsIgG, mouse immunoglobulin G; FITC, fluorescein isothiocyanate; PE, phycoerythrin; APC, allophycocyanin; BV, Brilliant Violet; PerCP, peridinin chlorophyll protein; APC-H7, APC conjugated with H7 dye.

in this case. Southern blot analysis showed that T-cell receptor β-chain Jβ2, β-chain Jβ1, β-chain Cβ1, and γ-chain Jγ were rearranged, whereas T-cell receptor δ-chain Jδ1 was not clonally rearranged (Fig. 3). These findings typically indicate clonal expansion of mature T cells, which are generally considered to have a TCR-αβ–positive immunophenotype.

We considered MEITL for her diagnosis, and differential diagnosis included enteropathy-associated T-cell lymphoma (EATL), indolent T-cell lymphoproliferative disorder of the gastrointestinal tract, and other natural killer (NK)-cell lymphomas, such as extranodal NK/T-cell lymphoma (ENKL). EATL is commonly associated with celiac disease, and histopathology often reveals pleomorphic lymphoma cells composed of medium to large-sized cells, which are different from those observed in the present case. Moreover, an indolent T-cell lymphoproliferative disorder of the gastrointestinal tract follows a gradual course by definition, which was not consistent with her very aggressive presentation. In other NK-cell lymphomas, including ENKL, lymphoma cells demonstrate the presence of Epstein-Barr virus, which was not proven

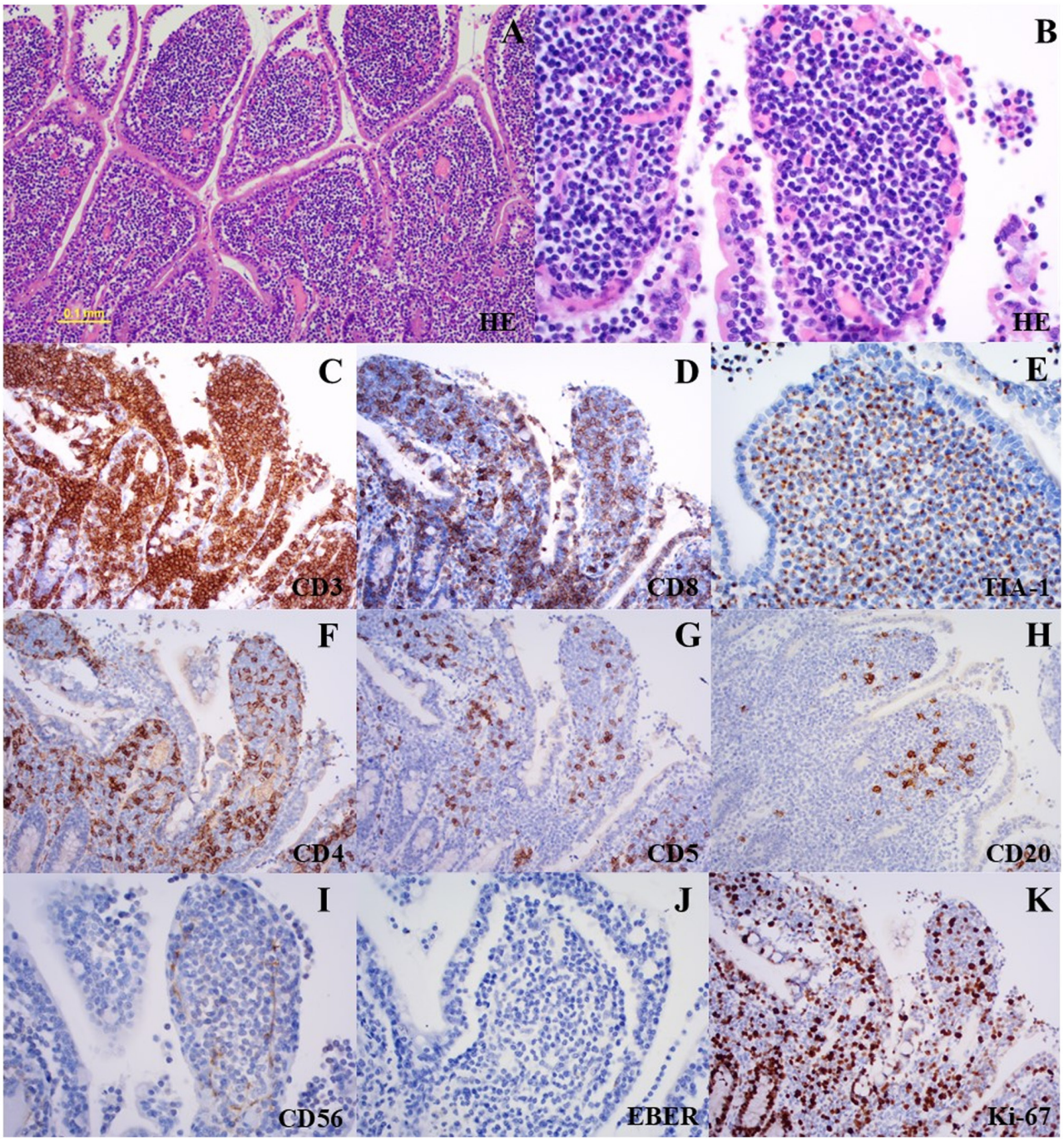

Figure 2. Histopathological findings. (A) Photomicrograph (magnification, x100) of the jejunum showing a dense infiltrate of monomorphic lymphocytes in all layers of the jejunum. (B) High-power photomicrograph (magnification, x400) demonstrating cytological uniformity of the infiltrating lymphocytes. Immunostaining is positive for (C) CD3, (D) CD8 and (E) TIA-1, and negative for (F) CD4, (G) CD5, (H) CD20, (I) CD56 and (J) EBER-ISH. (K) The Ki-67 proliferation index was approximately 40%. TIA-1, T-cell intracellular antigen-1; EBER-ISH: Epstein-Barr virus-encoded RNA-i*n situ* hybridization.

in her pathological analysis. Based on the absence of celiac disease, aggressive clinical course, and characteristic histopathological and immunophenotypic features, we could rule out enteropathy-associated T-cell lymphoma, indolent T-cell lymphoproliferative disorder of the gastrointestinal tract, and other NK-/T-cell lymphomas, and established a diagnosis of MEITL (5).

To determine the nature of the gallbladder mass, the patient underwent additional diagnostic tests. Positron emission tomography revealed radiotracer-avid lesions on the hepatic and intestinal surfaces (Fig. 1C). The mesentery and left adrenal gland were also involved, and the gallbladder mass was suspected to be infiltrated by MEITL (Fig. 1D). Abdominal ultrasound showed a hypoechoic gallbladder mass that was not deformed by body movement and had poor blood flow. Gallbladder wall thickening was observed in some areas, but the lamina structure was preserved (Fig. 4A-C). On magnetic resonance imaging (MRI), the gallbladder mass was iso-to-hypointense on T2-weighted images, hyperintense on diffusion-weighted images, and had a low apparent diffusion coefficient (ADC) value. Multiple gallstones were also observed (Fig. 4D-G).

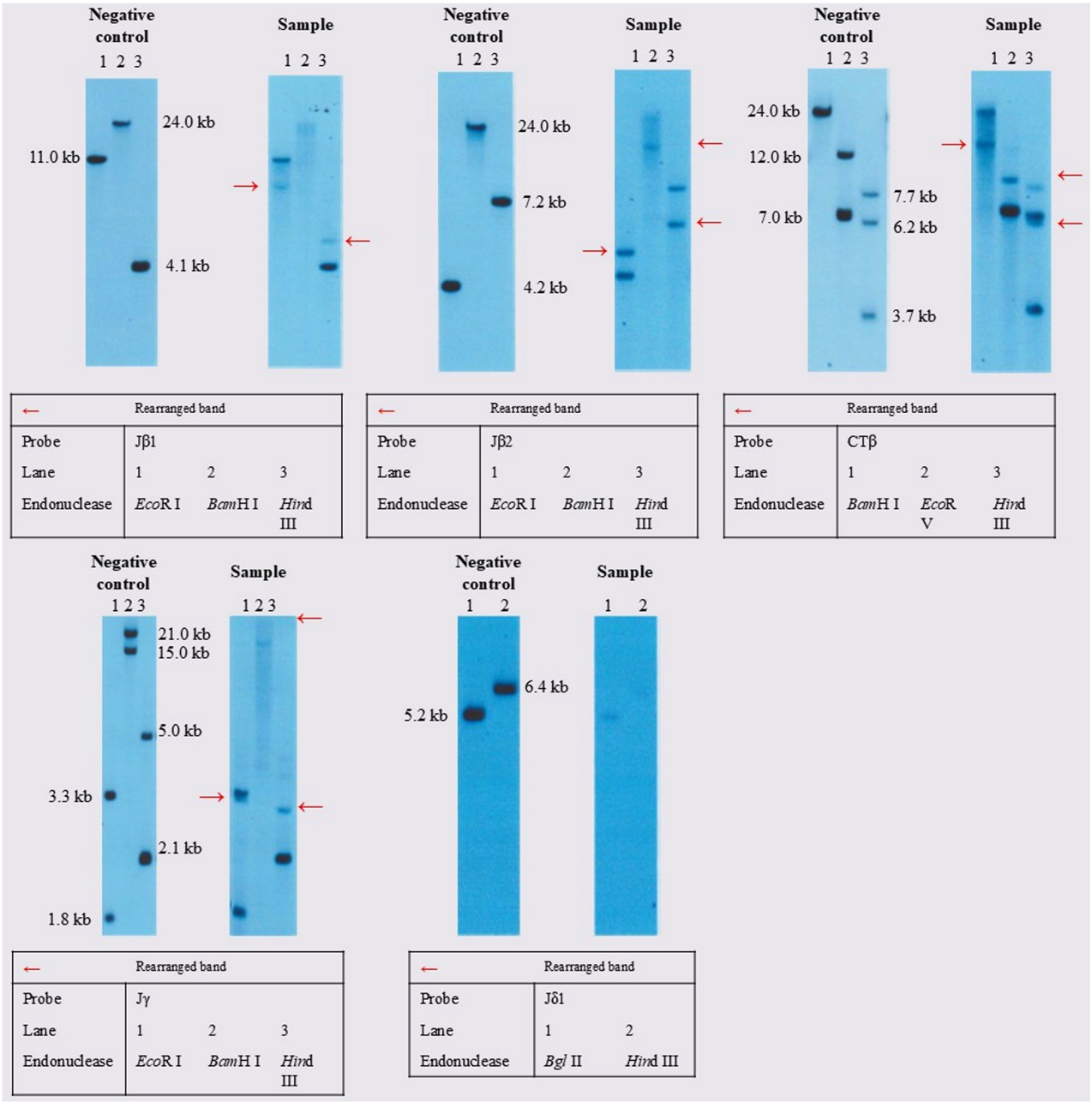

Figure 3. TCR rearrangement findings. Southern blot was performed as follows. i) DNA Extraction; ii) Restriction Enzyme Digestion. The common recognition sites for the restriction endonucleases used are as follows: *Eco*RI: 5'-GAATTC-3', *Bam*HI: 5'-GGGATCC-3', *Hind*III: 5'-AAGCTT-3'. iii) Electrophoresis; iv) Southern Transfer; v) Hybridization; vi) Chemiluminescent Detection; vii) Interpretation. In the negative control, bands corresponding to the nucleotides affected by the restriction enzymes are observed in each lane. Bands at a specific molecular weight correspond to the un-rearranged configuration. Other hand, bands that appear at alternative molecular weights indicate that rearrangement has occurred. The appearance of a distinct band (marked with a red arrow) in the sample, which is absent in the negative control, reflects a clonal rearrangement in the TCR gene. This rearranged band is evidence that the affected T-cells have undergone the rearrangement process, leading to the unique configuration associated with clonal expansion, as seen in T-cell lymphomas. T-cell receptor β-chain Jβ1, β-chain Jβ2, β-chain Cβ1, and γ-chain Jγ were rearranged. T-cell receptor δ-chain Jδ1 was not clonally rearranged. TCR, T-cell receptor.

These imaging findings raised suspicion of lymphoma; however, distinguishing it from gallbladder cancer based on imaging only was impossible. Nonetheless, a diagnosis of gallbladder lymphoma would have meant a significant risk of gallbladder perforation owing to chemotherapy. Therefore, following the reduction in drainage from the surgical site wound and the subsidence of the patient's fever and abdominal pain symptoms, 25 days post-admission, we performed a cholecystectomy (Fig. 1E). Histopathological analysis showed an infiltrate of monomorphic lymphocyte-like cells, similar to that in the jejunum lesion. Upon immunostaining, the abnormal lymphocytes were positive for CD3, CD8, and negative for CD4, CD5, CD20, CD56, and EBER-ISH (Fig. 5A-I). Flow cytometry results showed that the tumor cells were positive for CD3, CD7, CD8, CD38, CD56, and TCRαβ and negative for CD4, CD5, CD20, CD30, and TCRγδ (Fig. 6A). T-cell receptor β-chain Jβ2, β-chain Jβ1, β-chain Cβ1, and γ-chain Jγ were rearranged, whereas T-cell receptor δ-chain Jδ1 was not clonally rearranged (Fig. 6B). The rearranged band in the sample was consistent with that observed in the jejunum, suggesting that the tumor

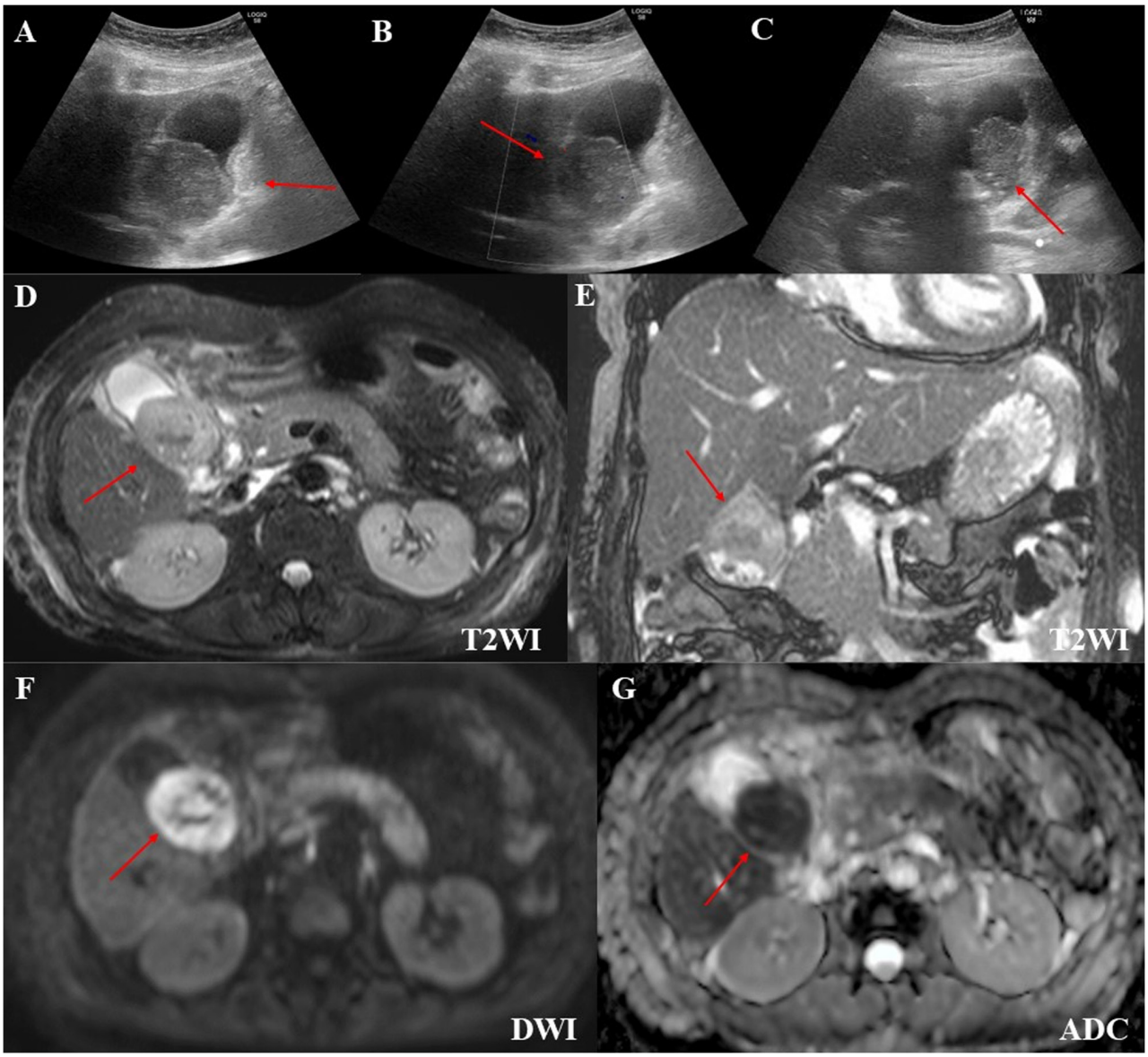

Figure 4. Gallbladder ultrasound findings and magnetic resonance imaging findings. Ultrasound showed a neoplastic lesion that was not deformed by body movement. (A) The arrow indicates thickening of the wall; however, the lamina structure was preserved. The mass (B) was hypoechoic and (C) had poor blood flow. (D) MRI showed a T2WI iso-low signal. (E) Multiple gallstones were observed. (F) DWI showed a high signal. (G) ADC map demonstrated a low value. DWI, diffusion-weighted imaging; ADC, apparent diffusion coefficient.

originated from the same clone. Karyotyping analysis was unavailable. We confirmed consistent histopathological findings in the jejunum and gallbladder tumors, leading to a diagnosis of MEITL with gallbladder involvement. Bone marrow aspirates and biopsy revealed no lymphoma cell involvement. Head CT and MRI showed no evidence of central nervous system (CNS) involvement. The patient's International Prognostic Index was 3, based on poor ECOG performance status, advanced stage, and extranodal lesions (6). Her Prognostic Index for T-cell lymphoma was 1, based on poor ECOG performance status (7).

Despite the surgical repair of the jejunum perforation on the day of admission, cholecystectomy 25 days after admission, and supportive care, her general condition continued to deteriorate; however, although her poor clinical condition was concerning, we considered that controlling the lymphoma was necessary. Therefore, 46 days after admission, chemotherapy was started according to the ifosfamide-cisplatin-etoposide (ICE) protocol, which resulted in marked tumor size reduction and improved her ECOG performance status. Considering the reported response rate of CHOP for MEITL is only about 40% (8) and the previous promising report of a Newcastle regimen for enteropathy-associated T-cell lymphoma (including MEITL) consisting of ifosfamide, etoposide, and epirubicin combined with autologous transplantation (9), we opted for ICE therapy instead. This therapy is routinely used at our institution, substituting a platinum agent for epirubicin because epirubicin is not typically used for lymphomas in Japan. Following three cycles of ICE therapy (10) (etoposide 100 mg/m^2 on days 1-3, carboplatin 650 mg/body, equivalent to the area under the curve=5 on day 2, and ifosfamide 5,000 mg/m^2 on day 2) and one cycle of cyclophosphamide-cytarabine (high-dose AraC)-dexamethasone-steroid-etoposide (CHASE) therapy (cyclophosphamide 1,200 mg/m^2 on day 1, Ara-C 2,000 mg/m^2 on days 2-3, etoposide 100 mg/m^2 on days 1-3,

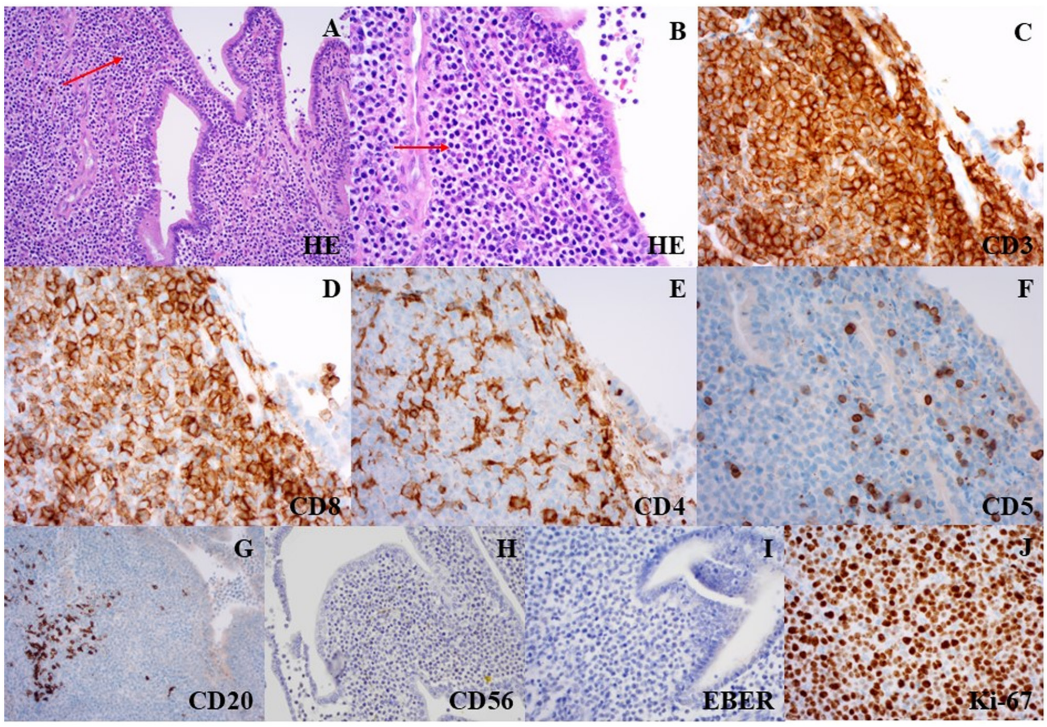

Figure 5. Gallbladder histopathological findings. (A) Photomicrograph (magnification, x100) of the gallbladder wall. The red arrow indicates an infiltrate of monomorphic lymphocyte-like cells similar to jejunum. (B) High-power photomicrograph (magnification, x400) highlighting the cytological uniformity of the infiltrating lymphoid cells. Immunostaining is positive for (C) CD3 and (D) CD8, and negative for (E) CD4, (F) CD5, (G) CD20, (H) CD56 and (I) EBER-ISH. (J) The Ki-67 proliferation index was approximately 90%.

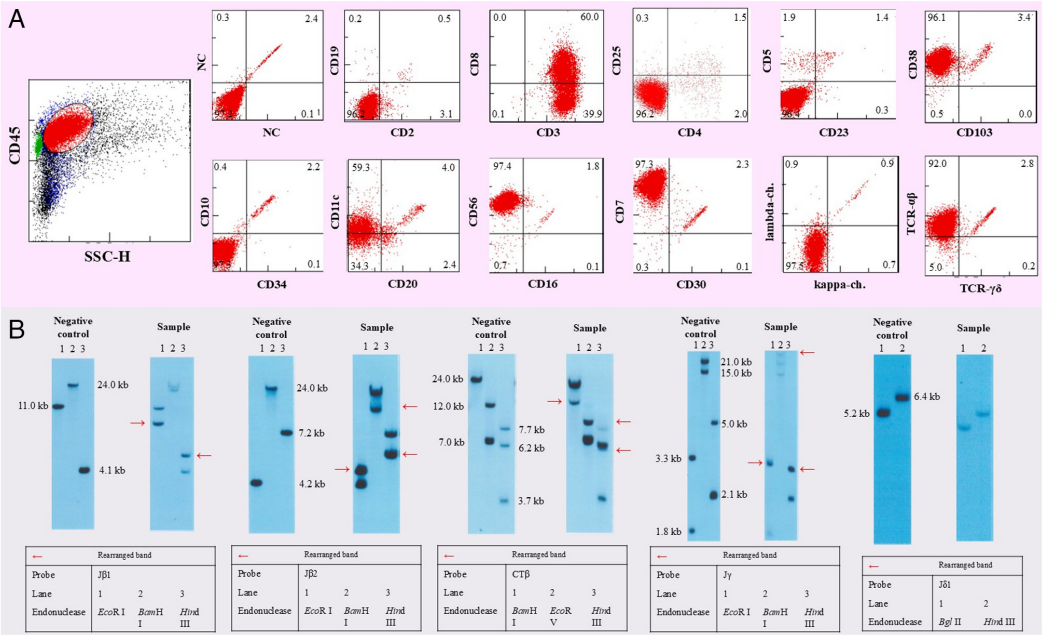

Figure 6. Flow cytometry and TCR rearrangement findings. (A) On flow cytometry, the tumor cells were positive for CD3, CD7, CD8, CD38, CD56, TCRαβ, and negative for CD4, CD5, CD20, CD30, and TCRγδ. (B) The appearance of a distinct band (marked with a red arrow) in the sample, which is absent in the negative control, reflects a clonal rearrangement in the TCR gene. This rearranged band is evidence that the affected T-cells have undergone the rearrangement process, leading to the unique configuration associated with clonal expansion, as seen in T-cell lymphomas. T-cell receptor β-chain Jβ1, β-chain Jβ2, β-chain Cβ1, and γ-chain Jγ were rearranged. T-cell receptor δ-chain Jδ1 was not clonally rearranged. TCR, T-cell receptor.

and dexamethasone 40 mg/body on days 1-3), a regimen developed in Japan specifically for stem cell harvesting (11). ICE and CHASE therapies are fully covered by insurance in Japan and are approved for this condition. We also referred to case reports from Japan (12,13) where autologous transplantation was performed after achieving complete remission (CR) with CHASE or ICE therapy. The patient underwent autologous peripheral blood stem cell transplantation and achieved

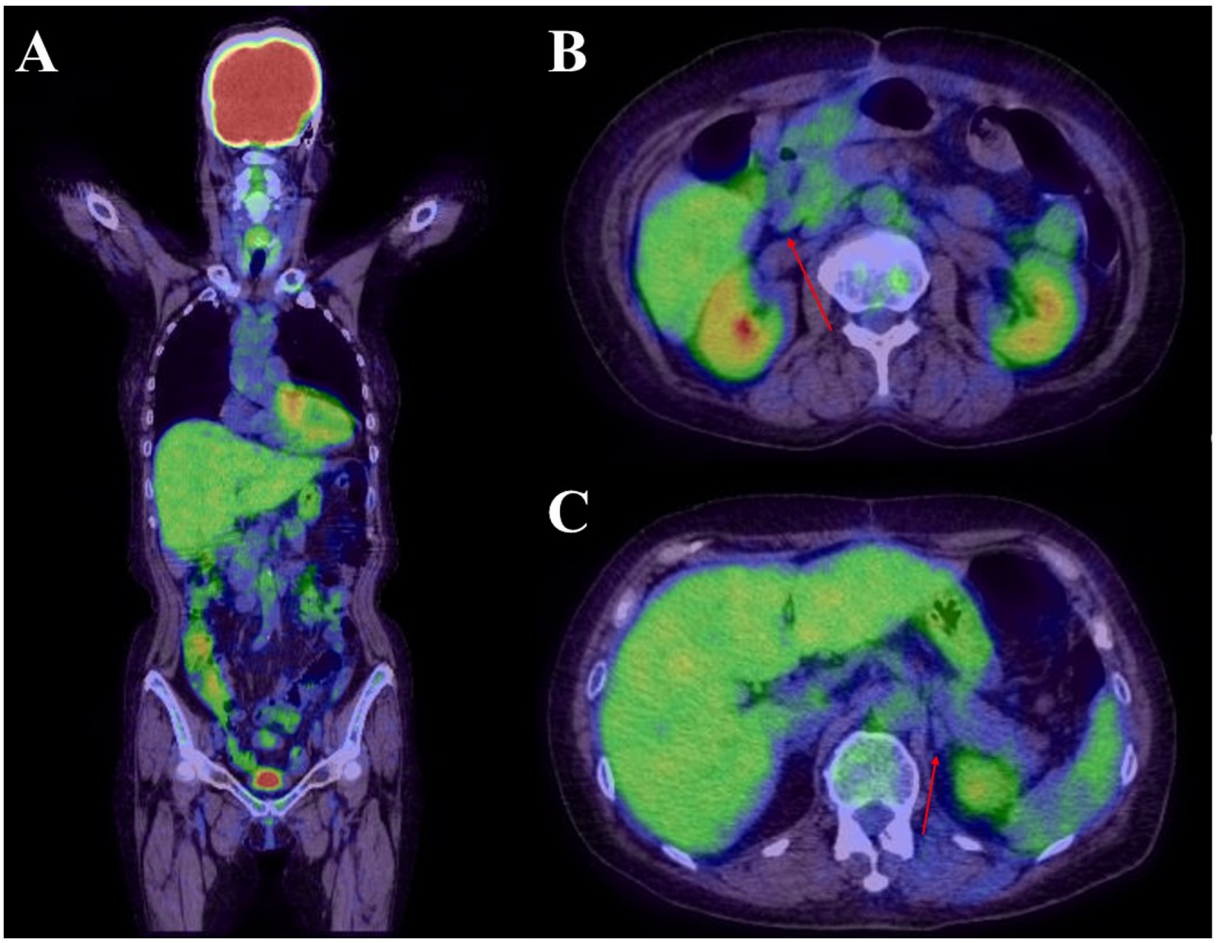

Figure 7. PET-CT images. (A) PET-CT scan showed no pathological FDG accumulation, including in the abdominal cavity. No FDG accumulation was observed in the (B) perihepatic region or the (C) adrenal glands. PET-CT, positron-emission tomography-computed tomography.

complete remission as confirmed by positron emission tomography (Fig. 7) in 233 days after admission. Unfortunately, she passed away 2 months after the transplantation owing to central nervous system recurrence.

Discussion

In this study, we presented a rare case of cooccurrence of two uncommon conditions in the same patient: a rare type of intestinal lymphoma and a previously unreported gallbladder invasion by MEITL. Cholecystectomy was beneficial both for establishing the diagnosis and completing chemotherapy safely, without chemotherapy-induced perforation.

Although gallbladder malignancies encompass a wide variety of malignant tumors, carcinomas constitute the majority of cases. Gallbladder lymphomas are uncommon, accounting for only 0.1-0.2% of all gallbladder malignancies because this organ does not usually contain lymphoid tissue (14). Two leading hypotheses have been introduced regarding the causes of lymphomagenesis in the gallbladder (15,16): i) lymph follicles formed owing to chronic inflammation, such as from gallstones, and ii) lymphoma from outside the gallbladder homing to the gallbladder wall through certain adhesive factors. In this case, identical cytomorphology was observed, suggesting that the lymphoma originating in the intestinal tract had infiltrated the gallbladder.

Most gallbladder lymphomas are of B-cell lineage, with mucosa-associated lymphoid tissue lymphoma and diffuse large B-cell lymphoma being the most commonly reported types. Although sporadic cases of other B-cell lymphomas arising from or involving the gallbladder have been reported (17-19), to the best of our knowledge, cases of gallbladder T-cell lymphomas, including MEITL, have not been documented.

Histopathological analysis of surgical specimens is the most accurate method for determining the nature of gallbladder masses. Imaging techniques such as ultrasound and MRI are less invasive and can also help differentiate between gallbladder carcinoma and lymphoma, including identifying lymphoma subtypes. However, the radiographic features of gallbladder MEITL remain unknown. On ultrasound, lymphoma lesions are typically confined to the submucosa, presenting with wall thickening and generally maintained lamina structure, as observed in this case. In contrast, gallbladder carcinoma often destroys the inner mucosal lamina (14,20-23). On MRI, malignant lymphomas and carcinoma demonstrate hyperintense signals on T2-weighted images and low ADC (15,17,20,24-28). In our case, the gallbladder mass demonstrated a low ADC but iso-to-hypointense T2-weighted signal. Among different lymphoma types, high-grade lymphomas, like diffuse large B-cell lymphoma, often form solid masses and cause irregular gallbladder wall

thickening on CT. Conversely, low-grade lymphomas, such as mucosa-associated lymphoid tissue lymphoma, follicular lymphoma, and small lymphocytic lymphoma, typically show mild wall thickening (14). In the present case, the gallbladder mass exhibited irregular wall thickening, resembling aggressive B-cell lymphomas.

In cases of suspected gallbladder lymphoma, cholecystectomy is vital not only for the diagnosis but also for the safe administration of chemotherapy and avoiding gallbladder perforation during treatment. Gastrointestinal lymphomas are also at high risk for perforation owing to progression and chemotherapy (29). Additionally, gallbladder perforation may occur. Thus, surgical resection is preferred for safe treatment (30), as illustrated in the present case.

There is no established treatment for MEITL. The National Comprehensive Cancer Network guidelines recommend a CHOP-like regimen as the first-line treatment for peripheral T-cell lymphomas. However, the reported response rate of CHOP for MEITL is only about 40% (8). Additionally, the efficacy of adding etoposide to CHOP therapy for T-cell lymphomas is still under debate (31). A 2010 study reported the successful use of a Newcastle regimen for enteropathy-associated T-cell lymphoma (including MEITL) consisting of ifosfamide, etoposide, and epirubicin combined with autologous transplantation (9). Since epirubicin is uncommonly used in Japan, we opted for ICE therapy, which is commonly employed at our institution. There have been reports from Japan of cases in which ICE or CHASE therapy, followed by autologous transplantation, resulted in complete remission (12,13). The patient responded well to the first course of ICE, prompting the administration of three courses. No CNS involvement was detected on head imaging, and CNS prophylaxis was not administered owing to concerns regarding treatment toxicity. Although CNS involvement in MEITL is rare (4), there have been cases where patients relapsed early post-transplantation, similar to our patient (32,33). Therefore, further investigations into optimal induction chemotherapy regimens and the necessity for CNS prophylaxis are warranted.

A limitation of this study is that TCR expression could not be assessed. Although we submitted a raw sample of the jejunal mass for flow cytometry, it was unsuitable for analysis, and results were unavailable.

In conclusion, we reported the first case of MEITL with gallbladder involvement. Despite the advances in imaging techniques, considering the low incidence of gallbladder lymphoma and previously reported cases of gallbladder lymphomas mimicking or coexisting with gallbladder carcinoma, cholecystectomy is still recommended as a diagnostic and therapeutic intervention. Following a definitive diagnosis, initiating prompt and appropriate treatment is imperative.

Acknowledgements

The authors would like to thank SRL, Inc. for performing the flow cytometry and Southern blotting.

Funding

No funding was received.

Availability of data and materials

The data generated in the present study may be requested from the corresponding author.

Authors' contributions

TO collected the data and wrote the first draft of the manuscript. TS performed pathological analysis. MN, YK, TT and MT provided hematological clinical information, including the disease course, therapeutic strategy selection and interpretation of hematological findings. MN and MT supervised the manuscript writing, editing, and review. JT and TI provided clinical information on surgical treatment and perioperative findings, including details of jejunum resection and the cholecystectomy. MT coordinated the project and edited the manuscript. MN and MT confirm the authenticity of all the raw data. All authors read and approved the final version of the manuscript.

Ethics approval and consent to participate

Not applicable.

Patient consent for publication

The patient's family provided written informed consent for the publication of their data and any related images.

Competing interests

The authors declare that they have no competing interests.

References

1. Delabie J, Holte H, Vose JM, Ullrich F, Jaffe ES, Savage KJ, Connors JM, Rimsza L, Harris NL, Müller-Hermelink K, *et al*: Enteropathy-associated T-cell lymphoma: clinical and histological findings from the international peripheral T-cell lymphoma project. Blood 118: 148-155, 2011.
2. Jantunen E, Boumendil A, Finel H, Luan JJ, Johnson P, Rambaldi A, Haynes A, Duchosal MA, Bethge W, Biron P, *et al*: Autologous stem cell transplantation for enteropathy-associated T-cell lymphoma: A retrospective study by the EBMT. Blood 121: 2529-2532, 2013.
3. Stuver R, Epstein-Peterson ZD and Horwitz SM: Few and far between: clinical management of rare extranodal subtypes of mature T-cell and NK-cell lymphomas. Haematologica 108: 3244-3260, 2023.
4. Yi JH, Lee GW, Do YR, Jung HR, Hong JY, Yoon DH, Suh C, Choi YS, Yi SY, Sohn BS, *et al*: Multicenter retrospective analysis of the clinicopathologic features of monomorphic epitheliotropic intestinal T-cell lymphoma. Ann Hematol 98: 2541-2550, 2019.
5. Hang JF, Yuan CT, Chang KC, Wang RC, Chen BJ, Hsieh PP, Huang WT, Chuang WY, Chen TW, Yeh YC, *et al*: Targeted next-generation sequencing reveals a wide morphologic and immunophenotypic spectrum of monomorphic epitheliotropic intestinal T-cell lymphoma. Am J Surg Pathol 46: 1207-1218, 2022.
6. International Non-Hodgkin's Lymphoma Prognostic Factors Project: A predictive model for aggressive non-Hodgkin's lymphoma. N Engl J Med 329: 987-994, 1993.
7. Gallamini A, Stelitano C, Calvi R, Bellei M, Mattei D, Vitolo U, Morabito F, Martelli M, Brusamolino E, Iannitto E, *et al*: Peripheral T-cell lymphoma unspecified (PTCL-U): A new prognostic model from a retrospective multicentric clinical study. Blood 103: 2474-2479, 2004.

8. Daum S, Ullrich R, Heise W, Dederke B, Foss HD, Stein H, Thiel E, Zeitz M and Riecken EO: Intestinal non-Hodgkin's lymphoma: a multicenter prospective clinical study from the German Study Group on Intestinal non-Hodgkin's Lymphoma. J Clin Oncol 21: 2740-2746, 2003.
9. Sieniawski M, Angamuthu N, Boyd K, Chasty R, Davies J, Forsyth P, Jack F, Lyons S, Mounter P, Revell P, *et al*: Evaluation of enteropathy-associated T-cell lymphoma comparing standard therapies with a novel regimen including autologous stem cell transplantation. Blood 115: 3664-3670, 2010.
10. Gisselbrecht C, Glass B, Mounier N, Singh Gill D, Linch DC, Trneny M, Bosly A, Ketterer N, Shpilberg O, Hagberg H, *et al*: Salvage regimens with autologous transplantation for relapsed large B-cell lymphoma in the rituximab era. J Clin Oncol 28: 4184-4190, 2010.
11. Ogura M, Yamamoto K, Morishima Y, Wakabayashi M, Tobinai K, Ando K, Uike N, Kurosawa M, Gomyo H, Taniwaki M, *et al*: R-high-CHOP/CHASER/LEED with autologous stem cell transplantation in newly diagnosed mantle cell lymphoma: JCOG0406 STUDY. Cancer Sci 109: 2830-2840, 2018.
12. Ishibashi H, Nimura S, Kayashima Y, Takamatsu Y, Aoyagi K, Harada N, Kadowaki M, Kamio T, Sakisaka S and Takeshita M: Multiple lesions of gastrointestinal tract invasion by monomorphic epitheliotropic intestinal T-cell lymphoma, accompanied by duodenal and intestinal enteropathy-like lesions and microscopic lymphocytic proctocolitis: A case series. Diagn Pathol 11: 66, 2016.
13. Umino A, Kubota Y, Honda-Yoshigai M, Okazaki T, Yoshihara Y, Wakayama K, Kawasaki S, Kusaba K, Kimura S and Sueoka E: Monitoring of tumor cells by flow cytometry permits rapid evaluation of disease progression in monomorphic epitheliotropic intestinal T-cell lymphoma. Cytometry B Clin Cytom 100: 454-456, 2021.
14. Ono A, Tanoue S, Yamada Y, Takaji Y, Okada F, Matsumoto S and Mori H: Primary malignant lymphoma of the gallbladder: A case report and literature review. Br J Radiol 82: e15-e19, 2009.
15. Mittal PK, Moreno CC, Kalb B, Mittal A, Camacho JC, Maddu K, Kitajima HD, Quigley BC, Kokabi N and Small WC: Primary biliary tract malignancies: MRI spectrum and mimics with histopathological correlation. Abdom Imaging 40: 1520-1557, 2015.
16. Dierlamm J, Baens M, Wlodarska I, Stefanova-Ouzounova M, Hernandez JM, Hossfeld DK, De Wolf-Peeters C, Hagemeijer A, Van den Berghe H and Marynen P: The apoptosis inhibitor gene API2 and a novel 18q gene, MLT, are recurrently rearranged in the t(11;18)(q21;q21) associated with mucosa-associated lymphoid tissue lymphomas. Blood 93: 3601-3609, 1999.
17. Hosoda K, Shimizu A, Kubota K, Notake T, Hayashi H, Yasukawa K, Umemura K, Kamachi A, Goto T, Tomida H, *et al*: Gallbladder Burkitt's lymphoma mimicking gallbladder cancer: A case report. World J Gastroenterol 28: 675-682, 2022.
18. Manesh M, Henry R, Gallagher S, Greas M, Sheikh MR and Zielsdorf S: Hodgkin lymphoma masquerading as perforated gallbladder adenocarcinoma: A case report. World J Gastrointest Surg 13: 1279-1284, 2021.
19. Kusunoki R, Fujishiro H, Yoshimura M, Sawada K, Suemitsu S, Kataoka M, Fujiwara A, Tsukano K, Kotani S, Yamanouchi S, *et al*: Intravascular large B-cell lymphoma mimicking hepatobiliary infection: A case report and literature review. Intern Med 58: 1885-1889, 2019.
20. Cocco G, Delli Pizzi A, Basilico R, Fabiani S, Taraschi AL, Pascucci L, Boccatonda A, Catalano O and Schiavone C: Imaging of gallbladder metastasis. Insights Imaging 12: 100, 2021.
21. Ayub A, Rehmani S, Al-Ayoubi AM, Lewis E, Santana-Rodríguez N, Raad W, Bhora F and Kim G: Primary non-Hodgkin's lymphoma of the gallbladder: A population-based analysis. Anticancer Res 37: 2581-2586, 2017.
22. Kalra N, Gupta P, Singhal M, Gupta R, Gupta V, Srinivasan R, Mittal BR, Dhiman RK and Khandelwal N: Cross-sectional imaging of gallbladder carcinoma: An update. J Clin Exp Hepatol 9: 334-344, 2019.
23. Honda M, Furuta Y, Naoe H and Sasaki Y: Primary mucosa-associated lymphoid tissue (MALT) lymphoma of the gallbladder and review of the literature. BMJ Case Rep 2017: bcr2017220161, 2017.
24. Psarras K, Symeonidis N, Vlachaki E, Baltatzis M, Papatolios G, Pavlidis E, Mouratidou C, Venizelos I, Pavlidis T, Sakantamis A and Nikolaidou C: Primary gallbladder small lymphocytic lymphoma as a rare postcholecystectomy finding. Case Rep Hematol 2014: 716071, 2014.
25. Rahim S, Ahmad Z, Chundriger Q, Ahmed A, Ali N and Abdul-Ghafar J: Secondary involvement of gallbladder by acute lymphoblastic leukemia presenting clinically as cholecystitis in a young patient: A case report. World J Surg Oncol 21: 63, 2023.
26. Mani H, Climent F, Colomo L, Pittaluga S, Raffeld M and Jaffe ES: Gall bladder and extrahepatic bile duct lymphomas: Clinicopathological observations and biological implications. Am J Surg Pathol 34: 1277-1286, 2010.
27. Furlan A, Ferris JV, Hosseinzadeh K and Borhani AA: Gallbladder carcinoma update: Multimodality imaging evaluation, staging, and treatment options. AJR Am J Roentgenol 191: 1440-1447, 2008.
28. Zemour J, Marty M, Lapuyade B, Collet D and Chiche L: Gallbladder tumor and pseudotumor: Diagnosis and management. J Visc Surg 151: 289-300, 2014.
29. Vaidya R, Habermann TM, Donohue JH, Ristow KM, Maurer MJ, Macon WR, Colgan JP, Inwards DJ, Ansell SM, Porrata LF, *et al*: Bowel perforation in intestinal lymphoma: Incidence and clinical features. Ann Oncol 24: 2439-2443, 2013.
30. Kato H, Naganuma T, Iizawa Y, Kitagawa M, Tanaka M and Isaji S: Primary non-Hodgkin's lymphoma of the gallbladder diagnosed by laparoscopic cholecystectomy. J Hepatobiliary Pancreat Surg 15: 659-663, 2008.
31. Wöhrer S, Chott A, Drach J, Püspök A, Hejna M, Hoffmann M and Raderer M: Chemotherapy with cyclophosphamide, doxorubicin, etoposide, vincristine and prednisone (CHOEP) is not effective in patients with enteropathy-type intestinal T-cell lymphoma. Ann Oncol 15: 1680-1683, 2004.
32. Nato Y, Miyazaki K, Imai H, Nakano E, Kageyama Y, Ino K, Fujieda A, Matsumoto T, Tawara I, Tanaka K, *et al*: Early central nervous system relapse of monomorphic epitheliotropic intestinal T-cell lymphoma after cord blood transplantation. Int J Hematol 114: 129-135, 2021.
33. Kubota Y and Kusaba K: Monomorphic epitheliotropic intestinal T-cell lymphoma involving the central nervous system. Blood 131: 1765, 2018.